Magnetic-susceptibility and specific-heat studies of spin-glass-like ordering in the pyrochlore compounds $R_2Mo_2O_7$ (R = Y, Sm, or Gd)

N. P. Raju, E. Gmelin, and R. K. Kremer
Max-Planck-Institut für Festkörperforschung, Heisenbergstrasse 1, 7000 Stuttgart 80, Federal Republic of Germany
(Received 30 March 1992)

Magnetic-susceptibility and specific-heat measurements have been performed on the cubic pyrochlore compounds $R_2Mo_2O_7$ (R = Y, Sm, or Gd). These compounds exhibit magnetic transitions at 18, 68, and 55 K, respectively, indicated by the magnetic-susceptibility data. Broad magnetic specific-heat anomalies, at the corresponding transition temperatures, suggest the absence of long-range magnetic ordering. The behavior of magnetic specific heat and magnetic entropy indicates that magnetic transitions in these compounds are due to spin-glass-like ordering of Mo^{4+} ions. The rare-earth ions in $Gd_2Mo_2O_7$ and $Sm_2Mo_2O_7$ appear to remain in a paramagnetic state down to 1.5 K and give rise to Schottky-like specific-heat anomalies at low temperatures. A model is presented to describe these anomalies quantitatively.

I. INTRODUCTION

The series of compounds $R_2Mo_2O_7$ (R = Nd, . . . , Yb and Y) belong to the family of pyrochlores with the general formula $A_2B_2O_7$.[1] These compounds crystallize in the face-centered-cubic structure with the space group $Fd\bar{3}m$. There are eight formula units per unit cell. Metal atoms A and B are located on the sites 16d and 16c, respectively, and two kinds of crystallographically different oxygens occupy the 48f and 8b sites. The $A_2B_2O_7$ structure is built up of slightly distorted BO_6 octahedra and AO_8 distorted cubes. Each of the metal atoms in these compounds forms a three-dimensional network of corner-sharing tetrahedra. Such an arrangement leads to a very high degree of magnetic frustration if the nearest-neighbor interactions are antiferromagnetic.

Many physical properties of the $R_2Mo_2O_7$ compounds and some of their solid solutions have been investigated.[2–14] It has been reported that $R_2Mo_2O_7$ (R = Nd, Sm, and Gd) are metallic and show spontaneous magnetization below 100 K.[4,5] The magnetic transition temperatures have been determined from the peaks in the ac susceptibility data as 96, 80, and 57 K, respectively.[6] An analysis of the temperature derivative of resistivity data reveals clear peaks at the transition temperatures. Powder neutron-diffraction studies on $Nd_2Mo_2O_7$ indicate long-range magnetic ordering with a ferrimagnetic arrangement of the Nd and Mo moments at liquid-helium temperatures.[7] $Tb_2Mo_2O_7$ is semiconducting and shows a magnetic transition at 25 K.[8] Short-range ordering of the Tb magnetic moments was concluded from the occurrence of diffuse magnetic scattering in neutron-diffraction studies at 8 K. The remaining samples in the $R_2Mo_2O_7$ series are semiconducting and do not exhibit any indication of cooperative magnetic ordering down to 4.2 K.[5,9]

The compound $Y_2Mo_2O_7$, where Mo^{4+} is the only magnetic ion, is semiconducting and shows a magnetic transition at about 18 K.[4,6,10,11] Spin-glass behavior was concluded from the characteristic splitting of the zero-field-cooled (ZFC) and field-cooled (FC) magnetic susceptibility curves below this temperature. Early specific-heat measurements as well as powder neutron-diffraction studies gave no indication of long-range ordering at low temperatures.[12] A broad Schottky-like specific-heat contribution with a maximum at about 12 K was detected and attributed to a parasitic amount of perovskite impurities. In view of the magnetization measurements, it is suggestive that this Schottky-like anomaly is associated to the spin-glass-like behavior of $Y_2Mo_2O_7$. Powder neutron-diffraction data of $Y_2Mo_2O_7$ are consistent with the fully ordered cubic pyrochlore structure.[13] Since no apparent crystallographic disorder is necessary and spin-glass behavior relies on the topological frustration of the Mo sublattice only, $Y_2Mo_2O_7$ is a very interesting magnetic system. We have therefore repeated the specific-heat study on $Y_2Mo_2O_7$ and compared it with that of the insulating nonmagnetic isostructural compound $Y_2Ti_2O_7$ in order to obtain the magnetic contribution to the heat capacity of $Y_2Mo_2O_7$.

To throw further light on the nature of magnetic ordering in the $R_2Mo_2O_7$ and particularly to study the magnetic interplay between Mo and R (R = Sm,Gd), detailed magnetic susceptibility and heat-capacity studies on $Sm_2Mo_2O_7$ and $Gd_2Mo_2O_7$ have been performed.

II. EXPERIMENTAL DETAILS

The polycrystalline samples of $R_2Mo_2O_7$ (R = Sm, Gd, and Y) have been prepared by a solid-state reaction. High-purity R_2O_3 powders (99.99%) were prefired at 1000 °C for 5 h and cooled down to room temperature before weighing them. R_2O_3 and MoO_2 powders have been taken in stoichiometric proportion and mixed thoroughly. The mixture was pressed into pellets and heated, in an alumina crucible, at 1400 °C for 24 h in argon atmosphere and then cooled down to room temperature. This procedure was repeated until power x-ray-diffraction pat-

terns revealed that the samples formed are single phase. The lattice constants of $Y_2Mo_2O_7$, $Gd_2Mo_2O_7$, and $Sm_2Mo_2O_7$ have been determined to be 10.25, 10.36, and 10.40 Å, respectively. These values are in excellent agreement with those of reported lattice constants.[5,9,14]

Magnetic data have been obtained from room temperature down to 5 K with a SQUID magnetometer (Quantum Design, San Deigo). The specific heat of the samples, in the form of pellets, has been measured in the temperature range from 1.5 to 150 K using fully automated quasiadiabatic calorimeters equipped with Pt or Ge thermometers.[15]

The measured specific heat, C_p, of the magnetic compounds comprises contributions from the lattice specific heat, C_l, and magnetic specific heat, C_m. Since the C_l and C_m contributions of a magnetic compound cannot be measured directly, the C_l has to be properly evaluated in order to separate out the C_m from total specific heat, C_p. For this purpose, the following procedure has been adopted.

The specific heat of insulating and nonmagnetic $Y_2Ti_2O_7$, which is isostructural to $R_2Mo_2O_7$, was measured. The variation of the Debye temperature, Θ_D, with respect to temperature was calculated for all samples according to the Debye function. The Debye temperature values obtained for the nonmagnetic material $Y_2Ti_2O_7$ were multiplied by a scaling factor such that the scaled Θ_D values of $Y_2Ti_2O_7$ and a given sample of $R_2Mo_2O_7$ were equal at higher temperatures (well above the magnetic transition temperatures) where magnetic contributions to specific heat become negligible. The values of different scaling factors used to evaluate the lattice specific heat of the magnetic compounds $Y_2Mo_2O_7$, $Gd_2Mo_2O_7$, and $Sm_2Mo_2O_7$ are 0.91, 0.82, and 0.80, respectively. The scaled Θ_D vs T of $Y_2Ti_2O_7$ was then converted back into specific heat against temperature which was used to represent the lattice specific heat of the corresponding magnetic compound. Then, for each sample, the estimated lattice specific heat was subtracted from the total specific heat to obtain the magnetic contribution.

III. RESULTS AND DISCUSSION

A. $Y_2Mo_2O_7$

The inverse magnetic susceptibility of $Y_2Mo_2O_7$ (uncorrected for closed-shell diamagnetism) against temperature is shown in Fig. 1. Zero-field-cooled and field-cooled susceptibility curves, which differ below the transition temperature, are shown in the inset. The magnetic transition temperature has been determined as 18(1) K from the peak of the ZFC susceptibility. In the paramagnetic region, the susceptibility data do not obey a Curie-Weiss law. The deviations that become increasingly apparent towards high temperatures were accounted for by adding a temperature-independent constant α to the Curie-Weiss form as given below:

$$\chi = \frac{C}{T-\Theta} + \alpha \ . \qquad (1)$$

α comprises closed-shell diamagnetic susceptibility,

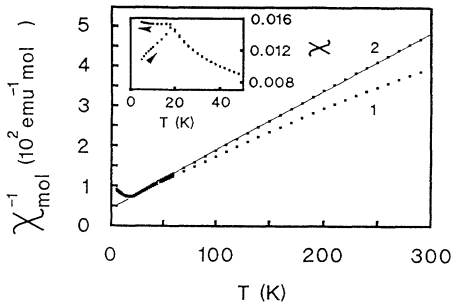

FIG. 1. Inverse of the measured susceptibility vs temperature for $Y_2Mo_2O_7$ (data points 1). Inverse of the corrected susceptibility (χ-α) against temperature (data points 2). The straight line is obtained according to Eq. (1). Inset shows ZFC and FC susceptibility data below 50 K.

$\chi_{dia}(-142\times10^{-6}$ emu mol^{-1}) and temperature-independent paramagnetic susceptibility χ_{TIP}. The best agreement of the susceptibility in the paramagnetic regime with (1) is obtained by using

$$\alpha = +450\times10^{-6} \text{ emu mol}^{-1}$$

or, correspondingly,

$$\chi_{TIP} = +592\times10^{-6} \text{ emu mol}^{-1} \ .$$

The effective magnetic moment was determined as $1.7\mu_B$ per Mo^{4+}. The paramagnetic Curie temperature Θ was found to be -28 K, indicating predominant antiferromagnetic exchange interactions. The effective magnetic moment of $\approx 1.7\mu_B$ phenomenologically indicates that the low-temperature magnetic behavior of Mo^{4+} is similar to that of a doublet with a powder-averaged g factor of ~ 2. Van Vleck–like contributions from excited states give rise to χ_{TIP} towards higher temperatures.

An effective moment of $\approx 1.7\mu_B$ represents a considerable reduction from $2.8\mu_B$, which is expected for a d^2 configuration leading to an $S=1$ triplet ground state. We ascribe this reduction of the effective moment to noticeable spin-orbit splitting effects of the 4d electrons. According to Kamimura *et al.*,[16] the effective Bohr magneton number for a $(d\epsilon)^2$ configuration in octahedral symmetry is significantly reduced if $k_BT < \xi_d$. The effective magnetic moment of Mo^{4+} varies from $1.5\mu_B$ to $2.0\mu_B$ if the spin-orbit coupling parameter ξ_d is about 10^3 cm^{-1}.[16] This is in good agreement with our experimental findings.

Measured specific heats, C_p, of $R_2Mo_2O_7$ (R = Y, Sm, and Gd) and the reference material $Y_2Ti_2O_7$, which is used for the construction of the lattice specific heat, are shown in Fig. 2. The comparison with the lattice specific heat of $Y_2Ti_2O_7$ reveals that extra specific-heat contributions, apparently of magnetic origin, are present at low temperatures. For $Y_2Mo_2O_7$ a broad magnetic specific-heat anomaly becomes clearly visible (Fig. 3) after subtracting the lattice part. The anomaly is centered around 20 K with a maximum value of 1.5 J mol^{-1} K^{-1}. Below about 15 K, C_m follows a linear temperature dependence:

$$C_m = 0.1\times T \text{ J mol}^{-1}\text{ K}^{-2} \text{ for } T < 15 \text{ K} \ .$$

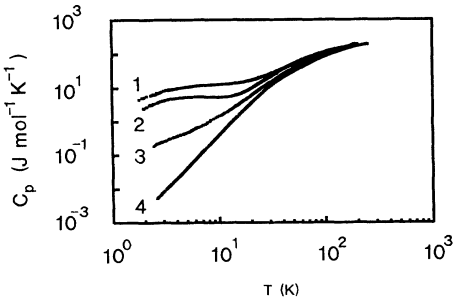

FIG. 2. Measured specific heat, C_p, for $Gd_2Mo_2O_7$ (data points 1), $Sm_2Mo_2O_7$ (data points 2), $Y_2Mo_2O_7$ (data points 3), and $Y_2Ti_2O_7$ (data points 4).

From the C_m data, we have obtained the magnetic entropy, S, as a function of temperature (Fig. 3) using the thermodynamic relationship

$$S(T)=\int_0^T \frac{C_m}{T'}dT' \ . \tag{2}$$

The magnetic entropy of $Y_2Mo_2O_7$ at the transition temperature, 18 K, is 1.6 or 0.8 J mol^{-1} K^{-1} for one formula unit of $YMoO_{3.5}$. The magnetic specific-heat and magnetic entropy data reveal the following remarkable features: (i) a broad anomaly in the C_m data with a maximum at about the spin-glass freezing temperature observed in the ZFC magnetic susceptibility, (ii) a linear temperature dependence of C_m below the transition temperature, and (iii) recovery of only about 14% of the expected magnetic entropy.

In particular, the linear variation of the low-temperature magnetic specific heat, suggesting a constant density of states of the low-temperature magnetic excitations, is claimed to be a common feature of spin glasses.[17,18] A linear behavior of the low-temperature magnetic specific heat was also observed for the related pyrochlore compound $Y_2Mn_2O_7$.[19] This compound shows many properties in common with spin glasses in spite of the fact that there is, as in $Y_2Mo_2O_7$, no evidence for chemical disorder.

A broad, smeared out, magnetic specific-heat anomaly is typically observed for spin glasses, indicating that short-range-order contributions extend up to very high temperatures.[20]

In summary, the thermal behavior of C_m substantiates the experimental results of the susceptibility and neutron diffraction in pointing to a spin-glass phase below 18 K in $Y_2Mo_2O_7$. The combination of the topology of the lattice and the predominant antiferromagnetic exchange interactions, as proven by the negative paramagnetic Curie temperature, appears to be responsible for the spin-glass behavior in $Y_2Mo_2O_7$.

B. $Sm_2Mo_2O_7$ and $Gd_2Mo_2O_7$

In $Sm_2Mo_2O_7$ and $Gd_2Mo_2O_7$, unlike in the case of $Y_2Mo_2O_7$, both the A and B metal sites are occupied by magnetic ions. Therefore, the magnetic behavior in these compounds is governed by inter- and intrasublattice exchange interactions of the corresponding rare-earth and molybdenum ions. ZFC and FC susceptibility data against temperature for $Gd_2Mo_2O_7$ and $Sm_2Mo_2O_7$ are shown in Fig. 4. Curie-Weiss parameters obtained from the high-temperature susceptibility data are compiled in Table I. Positive paramagnetic Curie temperatures of 53 and 101 K, observed for $Gd_2Mo_2O_7$ and $Sm_2Mo_2O_7$, respectively, in contrast to $Y_2Mo_2O_7$, indicate predominant ferromagnetic interactions. Below about 70 K for $Sm_2Mo_2O_7$ and about 57 K for $Gd_2Mo_2O_7$, the FC and ZFC susceptibility undergo a sharp rise that is very similar to that observed due to the onset of spontaneous long-range ordering in ferromagnetic materials. However, while the FC susceptibility saturates, the ZFC curves display a maximum and decrease towards low temperatures. For $Sm_2Mo_2O_7$, the ZFC susceptibility almost vanishes at very low temperatures. Field-dependent magnetization measurements at 5 K show saturation behavior. The values of saturation magnetic moments at 5 T for $Gd_2Mo_2O_7$ and $Sm_2Mo_2O_7$ are $14.7\mu_B$ and $2.2\mu_B$, re-

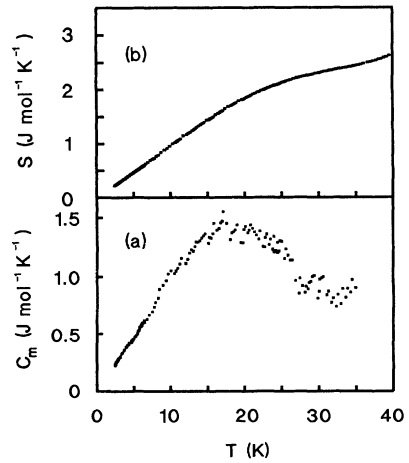

FIG. 3. (a) Magnetic specific heat, C_m, in $Y_2Mo_2O_7$. (b) Magnetic entropy vs temperature.

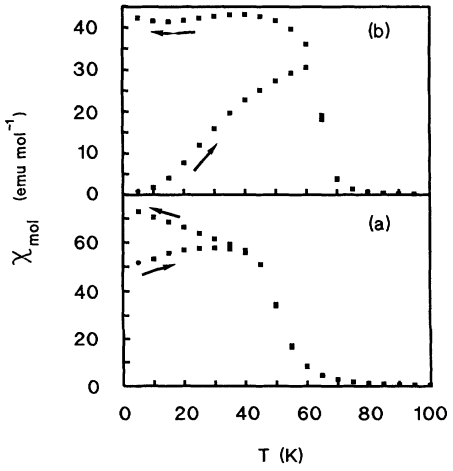

FIG. 4. (a) ZFC and FC susceptibility curves for $Gd_2Mo_2O_7$. (b) ZFC and FC curves for $Sm_2Mo_2O_7$.

TABLE I. Curie parameters of the compounds $R_2Mo_2O_7$ (R = Y, Sm, and Gd).

Sample	T_c (K)	Θ (K)	Curie constant, C (emu mol^{-1} K^{-1})	Effective magnetic moment (μ_B)
$YMoO_{3.5}$	18	−28	0.35	1.7
$SmMoO_{3.5}$	70	101	0.55	2.1
$GdMoO_{3.5}$	57	53	7.80	7.7

spectively, in good agreement with previous investigations.[6]

The specific heat of $Sm_2Mo_2O_7$ and $Gd_2Mo_2O_7$ (Fig. 2) display broad anomalies below about 30 K, apparently of magnetic origin. However, at first glance, no obvious magnetic anomaly can be seen around the temperature where the steep increase of the susceptibilities is observed. This finding rules out long-range ferromagnetic ordering as the origin of the sharp rise in the magnetization. Magnetic specific heat, C_m, of $Sm_2Mo_2O_7$ and $Gd_2Mo_2O_7$ have been obtained according to the procedure described in Sec. II and are plotted in Fig. 5. Magnetic specific heat contains very broad, smeared out anomalies with the maxima centering around 60 and 70 K for $Gd_2Mo_2O_7$ and $Sm_2Mo_2O_7$, respectively. The low-temperature and high-temperature anomalies overlap neatly in the temperature ranges around 30 and 40 K for $Sm_2Mo_2O_7$ and $Gd_2Mo_2O_7$, respectively. The entropy of the magnetic anomalies for $Sm_2Mo_2O_7$ and $Gd_2Mo_2O_7$ have been calculated according to (2) and are shown in Fig. 5. To see the linear temperature dependence of the magnetic specific heat, C_m, at low temperatures, the data below 4 K are shown in Fig. 6. The magnetic entropy values corresponding to the low-temperature anomalies are obtained as 5.7 J mol^{-1} K^{-1} per formula unit of $SmMoO_{3.5}$ and 15.3 J mol^{-1} K^{-1} per formula unit of $GdMoO_{3.5}$. The entropies of the high-temperature

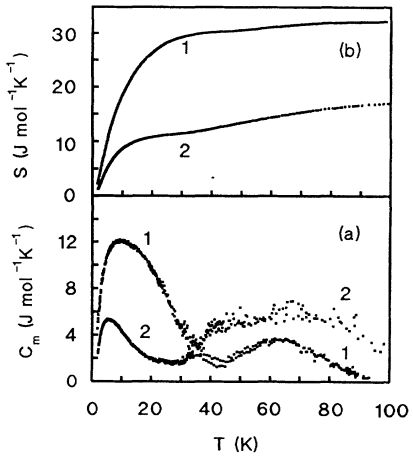

FIG. 5. (a) Magnetic specific heat, C_m, of $Gd_2Mo_2O_7$ (data points 1) and $Sm_2Mo_2O_7$ (data points 2). (b) Magnetic entropy, S, of $Gd_2Mo_2O_7$ (data points 1) and $Sm_2Mo_2O_7$ (data points 2).

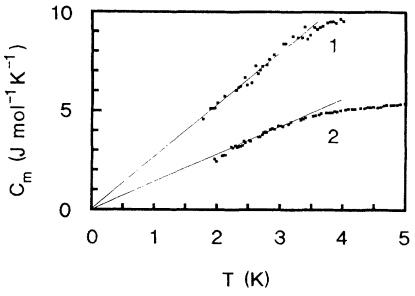

FIG. 6. Magnetic specific heat, C_m, of $Gd_2Mo_2O_7$ (data points 1) and $Sm_2Mo_2O_7$ (data points 2) below 4 K.

anomalies, up to the magnetic transition temperature, are significantly lower and amount to 1.8 J mol^{-1} K^{-1} per formula unit of $SmMoO_{3.5}$ and to 0.9 J mol^{-1} K^{-1} per formula unit of $GdMoO_{3.5}$. These entropy values are comparable to the entropy of the magnetic anomaly, up to the transition temperature, in $Y_2Mo_2O_7$ which is associated with the spin-glass ordering. These values are collected in Table II.

In summary, the heat-capacity studies on $Sm_2Mo_2O_7$ and $Gd_2Mo_2O_7$ leave us with the following intriguing result: The low-temperature Schottky-like anomaly has no corresponding feature in the magnetic susceptibility. The sharp rise of the susceptibility, however, is accompanied only by a very broad specific-heat anomaly. To understand the magnetic behavior of $Sm_2Mo_2O_7$ and $Gd_2Mo_2O_7$, we suggest the following.

The difference in ZFC and FC susceptibilities and the broad high-temperature specific-heat anomaly are indicative of spin-glass-like properties for $Sm_2Mo_2O_7$ and $Gd_2Mo_2O_7$. This spin-glass-like behavior of $Sm_2Mo_2O_7$ and $Gd_2Mo_2O_7$, as in $Y_2Mo_2O_7$, is induced by the Mo subsystem. Sizeable nearest-neighbor antiferromagnetic exchange in the Mo subsystem is a prerequisite to frustrate the Mo moments. However, the sharp-spontaneous-ordering-like increase of the magnetization and the sharp rise in the ac susceptibility manifest that considerable ferromagnetic correlations also occur in the Mo sublattice around the ordering temperature. They can be strongly enhanced by external magnetic fields and tend to align the rare-earth moments coupled ferromagnetically to the molybdem moments. Almost complete ferromagnetic saturation can be achieved in high external magnetic fields, particularly for $Gd_2Mo_2O_7$.

Here, it is worth mentioning a similar behavior that

TABLE II. Magnetic entropy values of $R_2Mo_2O_7$ (R = Y, Sm, and Gd) in different temperature ranges.

Sample	Temperature range in K	Entropy (J mol^{-1} K^{-1})
$YMoO_{3.5}$	0–18	0.8
$SmMoO_{3.5}$	0–30	5.7
	30–70	1.8
$GdMoO_{3.5}$	0–40	15.3
	40–57	0.9

was observed for $Y_2Mn_2O_7$.[19] $Y_2Mn_2O_7$ undergoes a magnetic transition at 20 K with a paramagnetic Curie temperature of +41 K. There is difference in ZFC and FC susceptibilities below T_c. Specific-heat data show no evidence for long-range magnetic ordering. Neutron-scattering studies indicate the presence of both antiferromagnetic (first neighbors) and ferromagnetic (second and third neighbors) short-range correlations. The authors attributed positive paramagnetic Curie temperature to the second- and third-neighbor ferromagnetic interactions. Saturation of the Mn moments also occurs in high magnetic fields.

We now turn our attention to the low-temperature specific-heat anomalies. The experimentally determined entropies for these anomalies are close to $Rln8$ for $Gd_2Mn_2O_7$ and $Rln2$ for $Sm_2Mo_2O_7$, indicating an eight-level magnetic ground state for $Gd_2Mo_2O_7$ and a two-level system for $Sm_2Mo_2O_7$. The anomalies have close resemblance to multilevel Schottky specific-heat anomalies. However, there are a number of distinct deviations.

(i) At low temperatures the specific-heat data increase linearly rather than exponentially, which is characteristic for Schottky anomalies.

(ii) The values of the maxima are significantly smaller than calculated for Schottky anomalies.

(iii) Particularly for $Gd_2Mo_2O_7$, the high-temperature tail of the magnetic specific heat falls off much steeper than $1/T^2$ as expected for a Schottky anomaly from a high-temperature expansion.

As already mentioned, there is no indication for magnetic ordering in the magnetic susceptibility data at low temperatures where the specific-heat anomalies are seen. It may also be noted that, for $Gd_2Ti_2O_7$, where Gd^{3+} is the only magnetic ion and the Gd-Gd distances are comparable to those in $Gd_2Mo_2O_7$, magnetic ordering is not observed down to 1 K.[21] In addition, we have also detected similar magnetic specific-heat anomalies at liquid-helium temperatures in other compounds $R_2Mo_2O_7$ (R =Dy, Ho, and Yb). Magnetic studies down to 1.5 K give no evidence of magnetic ordering in these systems.[22] From these findings we rule out that the low-temperature heat-capacity anomalies are due to magnetic ordering of the Gd or Sm moments. We rather suggest the following picture to understand the origin of these low-temperature anomalies.

Sm^{3+} (electronic configuration $4f^5$) develops a Kramer's doublet magnetic ground state because the six-fold degeneracy of the $^6H_{5/2}$ ground state is lifted by crystal-field-splitting effects. Gd^{3+} ion has a ground state $^8S_{7/2}$ and it is not much affected by crystal electric fields. It is known that this ground state is usually split by a Kelvin or less by zero-field-splitting effects.[23] Apart from crystal electric fields, the molybdenum–rate-earth exchange interaction generates a molecular field at the rare-earth sites. The molecular field lifts the degeneracy of the magnetic ground states of Gd and Sm (degeneracy 8 and 2, respectively). Due to the spin-glass-like behavior in the Mo sublattice of $Gd_2Mo_2O_7$ and $Sm_2Mo_2O_7$, the molecular field imposed on the rare-earth ions has random character. Consequently, instead of a well-defined molecular-field value, a field probability distribution is appropriate similar to the model used by Brout and Klein,[24] to describe the magnetic properties of dilute metallic spin glasses.

We now present a quantitative description of the low-temperature specific-heat anomalies. The magnetic specific heat, C_m, of an n-level Schottky system is obtained according to

$$C_m(T)=k_B\beta^2\frac{F(0)F(2)-F^2(1)}{F^2(0)}\ , \tag{3}$$

where k_B is the Boltzmann factor, $\beta=1/k_BT$, and $F(x)$ is defined by

$$F(x)=\sum_i E_i^x\exp(-\beta E_i)\ , \tag{4}$$

where $x=0,1,2$ and E_i is the Zeeman energy of the ith magnetic level

$$E_i=i\Delta \tag{5}$$

with $i=0,1$ for Sm and $i=0,1,\ldots,7$ for Gd. Δ is the energy difference between the two magnetic levels.

We assume a probability distribution for the splitting Δ to model the stochastic nature of the molecular field originating from the Mo spin-glass subsystem. Averaging the specific heats with this field distribution yields

$$\bar{C}_m(T)=\int_{-\infty}^{+\infty}P(\Delta')C_m(T,\Delta')d\Delta' \tag{6}$$

with $P(\Delta')$ being the normalized distribution of the splitting.

In order to fit the experimental data, both a simple rectangular distribution with cutoff σ,

$$P(\Delta')=C\begin{cases}1 & \text{for } -\sigma_R<\Delta'<\sigma_R\ ,\\ 0 & \text{elsewhere}\ ,\end{cases} \tag{7}$$

and a Gaussian probability distribution shifted by Δ_0,

$$P(\Delta')=C\begin{cases}\exp[-(\Delta'-\Delta_0)^2/2\sigma_G^2] & \text{for } \Delta'\geq 0\ ,\\ \exp[-(\Delta'+\Delta_0)^2/2\sigma_G^2] & \text{for } \Delta'<0\ ,\end{cases} \tag{8}$$

where C is the normalization factor defined by

$$\int_{-\infty}^{+\infty}P(\Delta')d\Delta'=1\ , \tag{9}$$

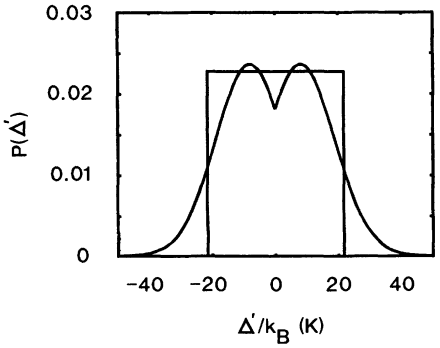

FIG. 7. Rectangular and Gaussian probability distributions obtained from Eqs. (7) and (8), respectively.

were tested as a first approximation to the internal field distribution.

The probability distributions (7) and (8) are displayed in Fig. 7 using the parameters σ_R, σ_G, and Δ_0, as obtained by fitting (6), using (7) and (8), to the experimental results of $Sm_2Mo_2O_7$. In the case of $Sm_2Mo_2O_7$, application of (7) with σ_R as the only adjustable parameter already simulates satisfactorily the characteristics of the anomaly. Figure 8(a) displays a fit of (6), using the Gaussian distribution (8), to the experimental data of $Sm_2Mo_2O_7$.

To fit the specific-heat anomaly of $Gd_2Mo_2O_7$, it was found necessary to introduce a temperature dependence of the random exchange fields according to a power law

$$\Delta_0(T)=\Delta_0(1-T/T_S)^{\alpha}\ ,$$
$$\sigma_{R,G}(T)=\sigma_{R,G}(1-T/T_S)^{\alpha}\ . \tag{10}$$

Equation (10) takes into account the fact that exchange fields vanish in the paramagnetic regime. T_S therefore must be identified with the temperature where the sharp increase of the FC and ZFC magnetizations occur. The critical decay of the exchange fields is simulated by allowing the splitting parameters σ_R, σ_G, and Δ_0 to vary according to a power law with a mean-field critical parameter $\alpha=0.5$.

Figure 8(b) displays a fit to Eq. (6) to the experimental data of $Gd_2Mo_2O_7$ using the rectangular distribution (7). T_S was set to 50 K as implied by the susceptibility experiments.

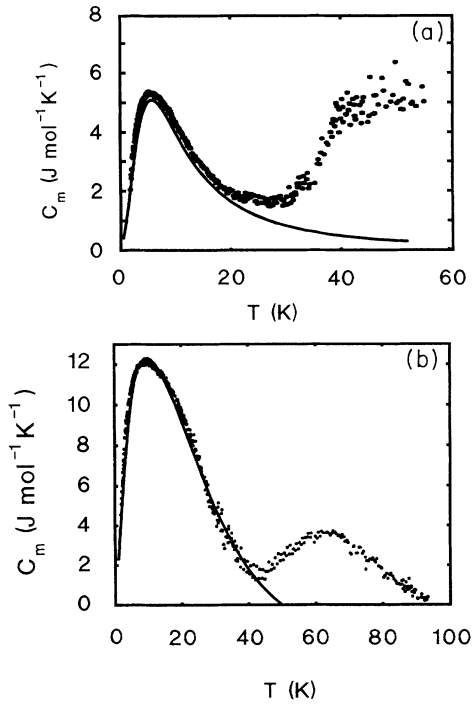

FIG. 8. (a) Magnetic specific heat, C_m, of $Sm_2Mo_2O_7$ (data points). The solid curve is obtained from a theoretical fit. See text for details. (b) Magnetic specific heat, C_m, of $Gd_2Mo_2O_7$ (data points). The solid curve is obtained from a theoretical fit. See text for details.

TABLE III. Compilation of parameters obtained from fits of our model to the low-temperature heat capacity of $Sm_2Mo_2O_7$ and $Gd_2Mo_2O_7$.

Sample	Δ_0	σ_G	σ_R
$Sm_2Mo_2O_7$	8	11	22
$Gd_2Mo_2O_7$	11	8	23

Table III compiles the parameters σ_R, σ_G, and Δ_0 obtained from the fits of (6) to the experimental data. The characteristic energy separation between consecutive magnetic levels (as given by σ_R, in the case of the rectangular distribution, and $\sigma_G+\Delta_0$ for the Gaussian distribution) is about 20 K and almost the same for both $Sm_2Mo_2O_7$ and $Gd_2Mo_2O_7$. This indicates that the exchange between rare-earth and moldybdenum moments is about the same in both compounds. The difference in paramagnetic Curie temperature by almost a factor of 2 (Table I) and the significantly higher-ordering temperature of $Sm_2Mo_2O_7$ point to a strong dependence of the Mo-Mo exchange on the particular host.

The formalism employed here to simulate the low-temperature specific heat of $R_2Mo_2O_7$ (R =Sm,Gd) was used in a similar manner to describe the specific heat of the spin-glass system $Eu_xSr_{1-x}S$.[25] There emphasis was layed on the linear specific heat at low temperatures.

Here we are able to follow in detail the full anomaly and it was unambiguously shown that a distribution of the exchange splittings is necessary to describe the rare-earth part of the specific heat of $R_2Mo_2O_7$ (R =Sm,Gd). It may also be viewed that rare-earth moments act as a probe to sense a random field distribution of the Mo spin-glass system. As a result of the present simulations we find that one characteristic parameter (width of the distribution, i.e., maximum possible splitting of the magnetic levels) is sufficient to simulate satisfactorily the distribution of exchange fields. The detailed shape of the particular probability is less critical. However, it is essential that the distribution is continuous to the lowest splitting energies (viz., a finite density of states for the lowest-energy magnetic excitations in the terminology of Ref. 25) to simulate the linear specific heat observed in the experimental data.

IV. SUMMARY

Magnetic transitions have been observed in the pyrochlore compounds $R_2Mo_2O_7$ (R =Y, Sm, and Gd) with differences in ZFC and FC susceptibility data. The absence of sharp λ-type anomalies in specific-heat data indicates that these transitions are not due to long-range magnetic ordering. Paramagnetic Curie temperatures suggest predominant antiferromagnetic interactions in $Y_2Mo_2O_7$ and ferromagnetic spin-spin correlations in $Sm_2Mo_2O_7$ and $Gd_2Mo_2O_7$. The splitting of the ZFC and FC susceptibility data below the transition temperatures also proves the presence of antiferromagnetic interactions in $Gd_2Mo_2O_7$ and $Sm_2Mo_2O_7$. A careful analysis of the

magnetic specific-heat behavior points out that the transitions in all these samples might arise due to spin-glass-like ordering of Mo moments.

The rare-earth ions, in $Sm_2Mo_2O_7$ and $Gd_2Mo_2O_7$, do not undergo any magnetic ordering and remain in paramagnetic state down to 1.5 K. Schottky-like specific-heat anomalies, at liquid-helium temperatures, have been observed in $Sm_2Mo_2O_7$ and $Gd_2Mo_2O_7$. Magnetic entropy values of $Sm_2Mo_2O_7$ and $Gd_2Mo_2O_7$ correspond to an eight-level and two-level system, respectively. These specific-heat anomalies can be understood as due to an exchange-induced splitting of the rare-earth magnetic levels. As a consequence of the spin-glass-like ordering of the Mo sublattice, the exchange fields at rare-earth sites are not unique. A simulation of the internal exchange field distribution, by simple rectangular or Gaussian probability distributions, allow the anomalies to be described.

ACKNOWLEDGMENTS

The authors would like to thank H. Bender for his help in preparing the samples and K. Ripka and E. Brücher for their assistance in calorimetric and magnetic measurements, respectively. One of the authors (NPR) gratefully acknowledges financial support from DAAD (German Academic Exchange Service).

[1]M. A. Subramanian, G. Aravamudan, and G. V. Subba Rao, Prog. Solid. State Chem. **15**, 55 (1983).

[2]A. Mandiram and J. Gopalakrishnan, Indian J. Chem. **19A**, 1042 (1980).

[3]R. Ranganathan, G. Rangarajan, R. Srinivasan, M. A. Subramanian, and G. V. Subba Rao, J. Low Temp. Phys. **52**, 481 (1983).

[4]J. E. Greedan, M. Sato, Naushad Ali, and W. R. Datars, J. Solid State Chem. **68**, 300 (1987).

[5]Mineo Sato, Xu Yan, and J. E. Greedan, Z. Anorg. Allg. Chem. **540-541**, 177 (1986).

[6]Naushad Ali, M. P. Hill, Sunil Labroo, and J. E. Greedan, J. Solid State Chem. **83**, 178 (1989).

[7]J. E. Greedan, J. N. Reimers, C. V. Stager, and S. L. Penny, Phys. Rev. B **43**, 5682 (1991).

[8]J. E. Greedan, J. N. Reimers, S. L. Penny, and C. V. Stager, J. Appl. Phys. **67**, 5967 (1990).

[9]N. P. Raju, G. Rangarajan, and R. Srinivasan, J. Phys. C **21**, 5427 (1988).

[10]N. P. Raju and G. Rangarajan, J. Phys.: Condens. Matter **2**, 3539 (1990).

[11]J. E. Greedan, M. Sato, Xu Yan, and F. S. Razavi, Solid State Commun. **59**, 895 (1986).

[12]K. Blacklock, H. W. White, and E. Gurmen, J. Chem. Phys. **15**, 1966 (1980).

[13]J. N. Reimers, J. E. Greedan, and M. Sato, J. Solid State Chem. **72**, 390 (1988).

[14]M. A. Subramanian, G. Aravamudan, and G. V. Subba Rao, Mater. Res. Bull. **15**, 1401 (1980).

[15]E. Gmelin and P. Roedhammer, J. Phys. E **14**, 223 (1981); E. Gmelin and K. Ripka, Cryogenics **21**, 117 (1981).

[16]H. Kamimura, S. Koide, H. Sekiyama, and S. Sugano, J. Phys. Soc. Jpn. **15**, 1264 (1960).

[17]L. E. Wenger and P. H. Keesom, Phys. Rev. B **11**, 3497 (1975); **13**, 4053 (1976).

[18]D. Meschede, F. Steglich, W. Felsch, H. Maletta, and W. Zinn, Phys. Rev. Lett. **44**, 102 (1980).

[19]J. N. Reimers, J. E. Greedan, R. K. Kremer, E. Gmelin, and M. A. Subramanaian, Phys. Rev. B **43**, 3387 (1991).

[20]J. A. Mydosh, in *Heidelberg Colloquium on Glassy Dynamics,* edited by J. L. van Hemmen and I. Morgenstern, Springer Lecture Notes in Physics, Vol. 275 (Springer, Berlin, 1987).

[21]J. D. Cashion, A. H. Cooke, M. J. M. Leask, T. L. Thoro, and M. R. Wells, J. Mater. Sci. **3**, 402 (1968).

[22]N. P. Raju, G. Gmelin, and R. K. Kremer (unpublished).

[23]A. Abragam and B. Bleaney, *Electron Paramagnetic Resonance of Transition Ions* (Oxford University Press, New York, 1970).

[24]M. W. Klein and R. Brout, Phys. Rev. **132**, 2412 (1963); M. W. Klein, **136**, A1156 (1964).

[25]U. Krey, Z. Phys. B **38**, 243 (1980).